Tellus SERIES B CHEMICAL AND PHYSICAL METEOROLOGY
PUBLISHED BY THE INTERNATIONAL METEOROLOGICAL INSTITUTE IN STOCKHOLM

Tellus (2011), 63B, 1040–1051

TELLUS

The dependence of soil H_2 uptake on temperature and moisture: a reanalysis of laboratory data

By D. H. EHHALT and F. ROHRER*, *Forschungszentrum Jülich, Institut IEK-8: Troposphäre, 52425 Jülich, Germany*

Manuscript received 7 April 2011; in final form 28 July 2011

ABSTRACT

In the past two types of laboratory experiments have been employed to determine the dependence of H_2 uptake by soils on temperature and moisture: Head space and flow experiments. The former actually measure the rate constant of the H_2 removal from the head space, k_H, the latter the uptake rate of H_2, U_{H2}, both caused by a given volume of soil. From an analytical solution of the diffusion equation in the soil we derive a mathematical relation between k_H and k_s, the desired uptake rate constant of H_2 in soil. Another equation relates U_{H2} with k_s. Both types of experiments actually determine the product of k_s with Θ_a, the air-filled pore volume fraction. $k_s \cdot \Theta_a$ for eolian sand and loess loam show zero uptake at very low and high moisture contents and a well defined maximum in between. Unlike soil moisture which also acts on the soil properties, the soil temperature, T, acts essentially on the enzyme activity only. Thus $k_s(T)$ is directly proportional to $k_H(T)$ or $U_{H2}(T)$ and the data of all experiments can be superimposed by scaling. The resulting average $k_s(T)$ shows a broad maximum around 30°C with zero uptake below −20°C and above 80°C.

1. Introduction

Molecular hydrogen, H_2, is a major trace gas of the global atmosphere. Although it is not a greenhouse gas, it has an impact on the atmosphere, since it is chemically reactive and thus affects the concentrations of ozone and hydroxyl radicals in the troposphere and stratosphere. Its atmospheric cycle, therefore, received renewed interest, when it became apparent that a future H_2 economy, which would be inevitably accompanied by additional emissions, might perturb the atmospheric H_2 budget and hence atmospheric chemistry (Tromp et al., 2003; Schultz et al., 2003; Warwick et al., 2004). The ensuing research on atmospheric H_2 confirmed an older finding, namely that the uptake of H_2 by soil constituted its major sink—with a rate of about 60 Tg yr^{-1} it contributes about 75% to the total sink strength—and that the large uncertainty in this sink constituted the major uncertainty in the H_2 budget (Novelli et al., 1999; Hauglustaine and Ehhalt, 2002; Sanderson et al., 2003; Rhee et al., 2006; Price et al., 2007; Ehhalt and Rohrer, 2009). Soil uptake of H_2 is certainly a topic that needs more attention.

H_2 uptake by soil appears to be widely spread. Virtually all soils containing organic carbon were shown to take up H_2. The uptake was shown to be a biological process—mediated by enzymes, that is, by various kinds of hydrogenase. For a long time the uptake was thought to be largely abiontic, that is, due to hydrogenase attached to soil particles or in dead cells, rather than to the metabolism of living cells (Conrad and Seiler, 1981; Conrad and Seiler, 1985; Schuler and Conrad, 1990; Conrad, 1999). Recent results have challenged that view and favour an uptake by living bacteria (Constant et al., 2010). In any case, sterilisation of the soil by heat or chemicals irreversibly destroys its capability for H_2 uptake.

The rate of uptake is usually expressed as deposition velocity, v_d (cm s^{-1}). The deposition velocities for H_2 were measured by numerous in situ experiments in various biomes and varied between 0.01 and 0.1 (cm s^{-1}) (see Ehhalt and Rohrer, 2009, for a summary). Nevertheless, the measurements did not suffice by far to characterize all soils, and the estimates of a global average soil uptake based on them involved large extrapolations. The field measurements generally showed a significant decrease of v_d with increasing soil moisture except occasional observations of very low v_d for very dry soils. The temperature dependence of v_d measured in the field was relatively weak and exhibited a broad maximum around 30°C (Liebl and Seiler, 1976; Conrad and Seiler, 1985; Förstel, 1986; Yonemura et al., 1999; Yonemura et al., 2000a, 2000b; Schmitt et al., 2009). Again the data were insufficient to characterize these dependencies for all relevant soils and situations.

There also exist a few laboratory measurements on the temperature and moisture dependence of H_2 uptake by soil. Made under controlled conditions they allow a precise choice and independent variation of the two parameters, and thus provide a

*Corresponding author.
e-mail: f.rohrer@fz-juelich.de
DOI: 10.1111/j.1600-0889.2011.00581.x

much clearer and more detailed description of these dependencies, albeit for a very limited selection of soils.

Two types of laboratory experiments have been employed for that purpose. The majority of the investigators used flask experiments, in which a soil sample was exposed to air containing H_2 at a mixing ratio around 500 ppb. The removal rate constant was determined by following the decay of the H_2 mixing ratio in the head space (Liebl and Seiler, 1976; Conrad and Seiler, 1981; Schuler and Conrad, 1991). Also in this category fall the measurements by Fallon (1982), who actually used tritiated hydrogen as tracer.

Another type of experiment used a flow system, in which air containing H_2 was pushed through a plug of soil. In this case the removal rate was determined from the difference in the H_2 mixing ratios of the ingoing and outgoing flow and the flow rate (Smith-Downey et al., 2006).

Besides a more precise definition of the dependencies, the laboratory experiments—especially the more systematic ones by Smith-Downey et al. (2006)—demonstrated that soil moisture and temperature act on the uptake rate independently of each other over a wide range of these two parameters, that is, their respective dependencies can be described by two separate functions.

As important as these measurements are, they are not directly applicable. What is needed for the modelling of v_d is the removal rate constant for H_2 within the soil itself (see Yonemura et al., 2000a). What the measurements provided was the rate constant for H_2 removal from the head space in the former and the removal rate of H_2 within the soil in the latter type of experiments. Both quantities are closely related, but not identical to the desired parameter, and may, therefore, show slightly modified dependencies on soil moisture and temperature.

In this paper, we will take a fresh look at the existing laboratory data. The primary aim is to provide realistic functional forms for the dependence of the rate constant of H_2 uptake in soil on temperature and moisture that will be of use for modelling v_d. A second aim is to obtain a clue on the absolute values of that rate constant. Since all of the published experiments were made on soil that had been manipulated, for example, by sieving, mixing, and aliquotting, and thus might not represent soil in its unperturbed state, the laboratory results may not be directly applicable to natural soils. Moreover, the publications do not provide all the data needed to transform the original data into the desired uptake rate constant and some—hopefully plausible—assumptions have to be made. This fresh look also provides some new insights that may help to encourage future laboratory or field experiments and to improve their design.

In the following two sections we will derive numerical expressions for the dependence of the H_2 uptake rate constant in the experimental soils—first on soil moisture, then on temperature. In a third section, we will discuss the results and their applicability to natural soils.

2. Dependence on soil moisture

There are three data sets available for that purpose (Conrad and Seiler, 1981; Fallon, 1982; Smith-Downey et al., 2006). Their results—in their original units—are summarized in Fig. 1.

Fallon (1982), employed 50 ml test tubes filled with 4–8 g (fresh weight) soil samples and tritiated H_2 (a mixture of HT and T_2 with less than 0.1 ppm of H_2 as carrier) and air in the headspace in his experiments. The mass-based soil moisture content was given in units of %w/w (weight water/dry weight soil). He investigated two types of soil: a coarse sand and sandy loam, and repeated the experiments about two weeks later. The results of the repeated runs did not agree. In the case of sand the second run, on 22 July, 1980, gave H_2 removal rate constants from the headspace, k_H, that were considerably lower then the k_H obtained in the first run, on 5 July, 1980. For a better comparison of the shape of the dependence the data from the second run were scaled by a factor of 1.68 in panel (a) of Fig. 1. In the case of sandy loam the k_H from the second run were substantially higher than those from the first; they are, therefore scaled by a factor of 0.33 in panel (b). In this case the shape of the second moisture dependence of k_H seems to differ significantly from the first one. The author also presented 1σ error bars for his measurements. They ranged up to $+40\%$, and for clarity are not given here.

The measurements by Conrad and Seiler (1981), were obtained from flask experiments placing 100 g (dry weight) of soil in a 1 l spherical bulb. The headspace was filled with air containing 0.7 ppm of H_2. Two types of soil were investigated: Eolian sand and loess loam. The data for eolian sand were collected in three runs: (1) Eolian sand in its original state; (a) water was added to reach the desired higher water contents, (b) the soil was allowed to dry to reach the lower water contents. (2) The soil samples were dried in air for 6 days; water was added to reach the required water contents. (3) The sand was dried for 60 days; water was added to reach the desired water contents. Run (2) and even more so run (3) showed decreased H_2 uptakes. In Fig. 1, panel (c) the values for run (2) and (3) are, therefore, scaled by a factor of 1.63 and 2.6, respectively, for better comparability. These scaling factors were obtained by matching the maximum values of the various runs. Since these maxima occurred at slightly different soil moistures, this procedure tends to broaden the shape of the maximum in the combined curve. Obviously there is little scatter in the data, and the shapes of the moisture dependences from the three runs are in excellent agreement.

The data for loess loam are from a single run (Fig. 1, panel d). This soil was dried in air for 10 d, then water added to reach the intended moisture content, which—as for eolian sand—is given in %w/w.

As mentioned before, the measurements by Smith-Downey et al., (2006) were made in a flow experiment. The pertinent parameters, which we will also need for our later evaluation, are: Soil volume, $V_s = 10\ cm^3$; H_2 mixing ratio in the incoming

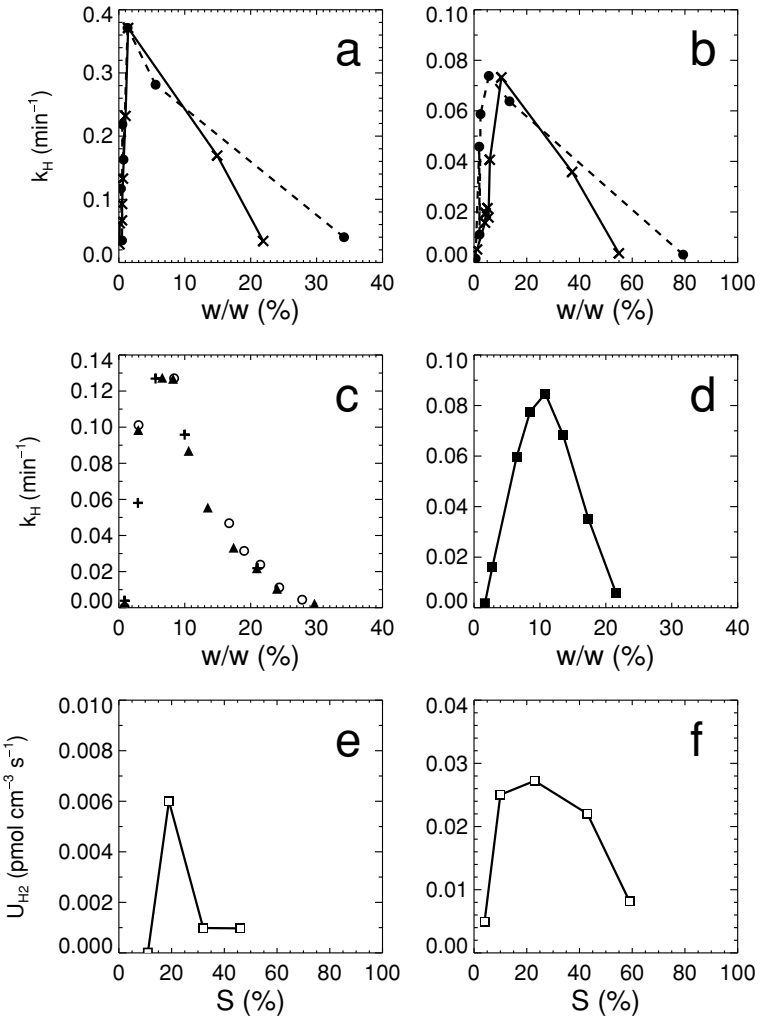

Fig. 1. H_2 removal rate constants from headspace, k_H, and H_2 uptake rates, U_{H2}, from flow experiments as a function of soil moisture. Panel a: coarse sand; crosses represent data from the 5 July, 1980 experiment, the full circles from the 22 July, 1980 experiment (Fallon, 1982). The latter are scaled by a factor of 1.68. Panel b: sandy loam; crosses: 5. July, 1980 experiment, full circles: 22 July experiment (Fallon, 1982). The latter are scaled by a factor of 0.33. Panel c: eolian sand from three experiment runs (Conrad and Seiler, 1981): Open circles: No treatment; full triangles: sand dried for 6 d prior to experiment, scaled by a factor of 1.63; crosses: sand dried for 60 d prior to experiment, scaled by a factor of 2.6. Panel d: loess loam (Conrad and Seiler, 1981). Panel e: sand (Smith-Downey et al., 2006). Panel f: boreal forest soil (Smith-Downey et al., 2006). In Panels e and f the moisture content is given as saturation, S. For more details see text.

air, $M_{in} = 1585 \pm 21$ ppb; air pressure, $p = 1.013 \times 10^5$ Pa; air flow rate, $f = 0.1667$ cm^{3}s^{-1}. From the outgoing H_2 mixing ratio, M_{out} the authors then calculated a H_2 uptake rate, U_{H2}, in units of pmol cm^{-3}s^{-1} using the expression

$$U_{H2} = \frac{(M_{in} - M_{out}) \cdot f \cdot p}{V_S \cdot R \cdot T \times 10^9}, \quad (1)$$

where R is the gas constant and T the temperature.

The soil moisture content was given as saturation, S, which the authors calculated from the ratio of the amount of water in the soil sample to the amount of water contained in the same soil after submerging it fully in water and allowing it to drain for 10 min. The authors investigated two soils: Soil from the Mojave Desert, a sand; and a soil from a boreal forest near Delta Junction, Alaska. That soil was not further characterized, except to say that it contained about 38% carbon. In case of the Mojave Desert soil a $S = 10\%$ corresponds to a soil moisture content of about 3.3% w/w, in the case of the boreal forest soil to about 4.6% w/w (Section 2.1). For better comparability with the other data in Fig. 1, which were made at room temperature, panels (e) and (f) show the data from Smith-Downey et al. (2006), made at 23°C.

The soil moisture dependences of the H_2 uptake rate, U_{H2}, or rate constant, k_H, displayed in Fig. 1 all agree in their broad outlines. (1) k_H and U_{H2} appear to vanish at very low moistures, approach zero at high moistures and show a well defined maximum in between. This general pattern has been explained on the basis that on the one side the enzymes responsible for the removal require a minimum of liquid water to be activated, and on the other that the transport of H_2 to the enzyme becomes blocked by water-filled pores at high soil moistures (Conrad and Seiler, 1981; Fallon 1982; Smith-Downey et al., 2006). (2) The increase of k_H and U_{H2} at low soil moistures is steeper than the decrease from the maximum at high soil moistures. (3) In all three data sets the maximum for sand is reached at lower soil moistures than that for the heavier soil (i.e. panels b, d, f).

A closer look, however, reveals also differences. The values for k_H obtained by Fallon (1982), for example never reach quite

zero, neither at the very low (∼0.01% w/w) nor the high soil moistures (>35% w/w). This is in contrast to the observations by Conrad and Seiler (1981), which indicate a $k_H = 0$ reached at 0.8% w/w for sand and at 1.7% w/w for loess loam, that is, a small but finite value for the cut-off at low moistures. They further strongly suggest that k_H approaches zero at about 30% w/w for sand and at about 23% w/w for loess loam at the high moisture end. The measurements by Smith-Downey et al. (2006), are to sparse to allow a firm conclusion, but they tend to support that aspect of the data by Conrad and Seiler (1981).

This points to a possible drawback in the use of tritiated H_2 in determining the uptake rate of H_2. Besides the uptake of H_2 and its conversion to H_2O, hydrogenase also catalyses an isotopic exchange

$$HT + H_2O \rightarrow HTO + H_2 \tag{2}$$

in which the isotopic signature is removed but no H_2 is lost. Thus, as Fallon (1982) himself pointed out the measurements using HT may not be directly applicable to the uptake of H_2. In fact they should represent an upper limit only. Since it is also not clear, what the exact size of his soils samples were for his various runs, a parameter which is needed for our re-evaluation, his data cannot be reanalyzed. We will, therefore concentrate our reanalysis on the data of Conrad and Seiler (1981), and the data of Smith-Downey et al. (2006), for boreal forest soil. Smith-Downey's measurements for sand show occasional negative H_2 uptake rates. The authors assign these to measurement errors. However, they could also be indicative of H_2 formation in the soil samples which would bias the observed uptake rates of H_2 especially at low moistures.

2.1. *Reanalysis of the headspace experiments*

To obtain the desired rate constant for the H_2 uptake within the soil, k_s, we note that all the removal takes place in the soil. Therefore, the rate of H_2 loss in the head space equals the rate of H_2 lost in the soil:

$$M_H \cdot V_H \cdot \rho \cdot k_H = k_S \cdot \overline{M_S} \cdot \rho \cdot \Theta_a \cdot V_S \tag{3}$$

and

$$k_s \cdot \Theta_a = k_H \cdot M_H / \overline{M_S} \cdot V_H / V_S. \tag{4}$$

Here M_H is the H_2 mixing ratio in the head space, $\overline{M_S}$ the average H_2 mixing ratio in the soil air; V_H and V_S are the volumes of the head space and soil, and ρ is the number density of air. Θ_a is the volume fraction taken up by air filled pores in the soil. It is given by

$$\Theta_a = \Theta_p - \Theta_w, \tag{5}$$

where Θ_p is the total porosity of the soil (cm^3 total pore space/cm^3 soil), Θ_w is the volumetric moisture content (cm^3 of water filled pores/cm^3 soil). The preparations of the experimental soils should have remove aggregation and dead pore volume, that is, pore volume inaccessible to H_2.

Since $\overline{M_S} < M_H$

$$k_s \cdot \Theta_a > k_H \frac{V_H}{V_S}. \tag{6}$$

Expressions (4) and (6) demonstrate that the measured k_H for the headspace does not map the moisture dependence of k_s, the rate constant for H_2 removal in the soil, but rather that of the product $k_s \cdot \Theta_a$, where Θ_a itself depends on the soil moisture. In fact $k_s \cdot \Theta_a$ is further modified by $\overline{M_S}/M_H$ which also depends on the soil moisture albeit more weakly than Θ_a (Section 2.1 below). The only firm conclusion at this point is that k_H multiplied by V_H/V_s, which is on the order of 10 for the considered experiments, provides a lower limit for $k_s \cdot \Theta_a$. To proceed we have to determine $\overline{M_S}/M_H$ and its dependence on soil moisture, which means we have to calculate the distribution of M_s in the soil.

Following Yonemura et al. (2000a) we assume that molecular diffusion drives the transport of H_2 within the soil. We further assume that our problem is primarily one-dimensional, that there is no production of H_2 in the soil and that the destruction is first order in the H_2 concentration. Then the diffusion equation takes the form:

$$\Theta_a \cdot \rho \cdot \frac{\partial M_S(z,t)}{\partial t} = \frac{\partial}{\partial z} P \cdot \rho \cdot \frac{\partial M_S(z,t)}{\partial z} - \rho \cdot k_s \cdot \Theta_a \cdot M_S(z,t), \tag{7}$$

where ρ is the number density of soil air in molec cm^{-3}, and z is the depth in cm. P is the diffusivity of H_2 in the soil (units: $cm^2\ s^{-1}$). There are different ways to calculate P. Here we choose the formulation by Millington and Quirk (1961)

$$P = \frac{\left(\Theta_p - \Theta_w\right)^{3.1} \cdot D}{\Theta_p^2} \tag{8}$$

(see also Yonemura et al., 2000a; Schmitt et al., 2009). Where D is the molecular diffusivity of H_2 in air (units: $cm^2 s^{-1}$). D depends on temperature, T in °C, and atmospheric pressure, p in hPa:

$$D = \frac{0.611 \times 1013.25}{p \cdot \left((T + 273.15)/273.15\right)^{1.75}} \tag{9}$$

(Yonemura et al., 2000a).

Our calculations will assume uniform soil conditions, that is, constant values for Θ_a, ρ, P, k_s. This is plausible because the experiments were designed to provide uniform soil conditions.

The boundary conditions are: $M_S(0, t) = M_H(t)$ at the soil surface and

$$F_s(z_L,t) = \rho \cdot P \cdot \frac{\partial M_s(z,t)}{\partial z}|_{z_L} = 0 \tag{10}$$

at the lower boundary, z_L, where the vertical H_2 flux, F_s, is blocked by the wall of the flask.

The temporal dependence of $M_H(t)$, which is given by the exponential decay, $M_H(t) = M_H(0) \cdot e^{-k_H \cdot t}$, suggests a solution of the form:

$$M_S(z,t) = M_H(0) \cdot m_S(z) \cdot e^{-k_H \cdot t}. \tag{11}$$

Inserting eq. (11) in the diff. eq. (7) and rearranging the terms we obtain:

$$\frac{\partial}{\partial \mathrm{z}}\rho \cdot P \cdot \frac{\partial m_{\mathrm{S}}(z)}{\partial z} - \rho\Theta_{\mathrm{a}}(k_{\mathrm{S}} - k_{\mathrm{H}})m_{\mathrm{S}}(z) = 0 \tag{12}$$

as differential equation for the spatial part, $m_{\mathrm{S}}(\mathrm{z})$.

With the given boundary conditions diff. eq. (12) has an analytical solution:

$$m_{\mathrm{S}}(z) = \frac{1}{1 + e^{2z_{\mathrm{L}}/\zeta}} \cdot \left\{ e^{2z_{\mathrm{L}}/\zeta} \cdot e^{-z/\zeta} + e^{z/\zeta} \right\}, \tag{13}$$

where $\zeta = \sqrt{\mathrm{P}/[\Theta_{\mathrm{a}} \cdot (k_{\mathrm{s}} - k_H)]}$ is the characteristic length of decrease in $m_{\mathrm{S}}(z)$, in units of cm, and $0 \le z \le z_{\mathrm{L}}$.

Integrating the resulting $M_{\mathrm{S}}(z,t)$ over $0 \le z \le z_{\mathrm{L}}$ we obtain the average $\overline{M_{\mathrm{S}}}$ in the soil at any given time:

$$\overline{M_{\mathrm{S}}}(t) = \frac{\zeta}{z_{\mathrm{L}}} \cdot \frac{e^{2z_{\mathrm{L}}/\zeta} - 1}{e^{2z_{\mathrm{L}}/\zeta} + 1} \cdot M_{\mathrm{H}}(t). \tag{14}$$

Hence eq. (4) turns into

$$k_{\mathrm{S}} \cdot \Theta_{\mathrm{a}} = k_{\mathrm{H}} \cdot \frac{V_{\mathrm{H}}}{V_{\mathrm{S}}} \cdot \frac{z_{\mathrm{L}}}{\zeta} \cdot \frac{(e^{2z_{\mathrm{L}}/\zeta} + 1)}{(e^{2z_{\mathrm{L}}/\zeta} - 1)}. \tag{15}$$

Since ζ is also a function of $k_{\mathrm{s}}{\cdot}\Theta_{\mathrm{a}}$, eq. (15) is an implicit equation for $k_{\mathrm{s}}{\cdot}\Theta_{\mathrm{a}}$.

It can be used to calculate $k_{\mathrm{s}}{\cdot}\Theta_{\mathrm{a}}$ provided we are able to determine the parameters, $V_{\mathrm{H}}, V_{\mathrm{s}}, z_{\mathrm{L}}$, as well as Θ_{p} and Θ_{w} which define P and Θ_{a}. These are not given in the paper by Conrad and Seiler (1981). But the soils are well enough characterized (Seiler et al., 1977) to obtain plausible and consistent estimates of these entities within relatively narrow bounds.

To estimate V_{S} and Θ_{p}, and further to convert the mass-based soil moisture into Θ_{w}, we have first to estimate the bulk density of the soil samples, ρ_{B}, which in turn requires estimates of the soil particle density ρ_{M}. The latter is 2.6 g cm^{-3} for eolian sand (based on a $\rho_{\mathrm{M}} = 2.65$ g cm^{-3} for sand and a contribution of 3% w/w of organic carbon) and 2.5 g cm^{-3} for loess loam (mainly due to its higher fraction of organic carbon of about 6%). ρ_{B} is related to ρ_{M} and Θ_{p}

$$\rho_{\mathrm{B}} = \rho_{\mathrm{M}} \cdot (1 - \Theta_{\mathrm{p}}), \tag{16}$$

where a term containing the density of air which is smaller by about 10^{-3} has been neglected on the right-hand side of eq. (16).

Θ_{w} is then given by

$$\Theta_{\mathrm{W}} = \mathrm{SM} \cdot \frac{\rho_{\mathrm{B}}}{\rho_{\mathrm{H_2O}}}, \tag{17}$$

where SM stands for the measured mass-based soil moisture in units of % w/w, and $\rho_{\mathrm{H2O}} = 1$ g cm^{-3} is the density of water.

By definition

$$\Theta_{\mathrm{p}} \ge \Theta_{\mathrm{W}}. \tag{18}$$

Expressions (16)–(18) allow to derive the inequality

$$\rho_{\mathrm{B}} \le \frac{\rho_{\mathrm{M}}}{1 + \mathrm{SM} \cdot \rho_{\mathrm{M}}}, \tag{19}$$

For eolian sand the experiments reached an k_{H} of virtually zero at a soil moisture content of 30% w/w (Fig. 1). Inequality (19) translates this soil moisture into an upper limit for ρ_{B}, namely $\rho_{\mathrm{B,es}} < 1.46$ g cm^{-3}. For loess loam the experiments reached only to 21.5% w/w, but at an finite k_{H}. Here we first have to extrapolate the curve for the moisture dependence of k_{H} to $k_{\mathrm{H}} = 0$ (Fig. 1, panel d). That extrapolation leads to a maximum soil moisture of 23% w/w for loess loam. The corresponding upper limit for ρ_{B} is $\rho_{\mathrm{B,ll}} = 1.59$ g cm^{-3}.

Due to the manipulation of the soil the samples in the flask experiments are expected to be more loosely packed than the soil in their natural setting. Consequently Θ_{p} should be larger. To capture the possible range in ρ_{B} and Θ_{p} in the experiments we calculate $k_{\mathrm{s}}{\cdot}\Theta_{\mathrm{a}}$ for several consistent pairs of (Θ_{p}; ρ_{B}): (0.44;1.46), (0.46;1.40), (0.50;1.30) for eolian sand, and (0.37;1.59), (0.40;1.50), (0.44; 1.40) for loess loam. The respective soil volumes, V_{s}, are obtained by dividing the dry weight of the soil samples, 100 g, by the respective ρ_{B}. The volume of the head space, V_{H}, is (1000 – V_{s}) cm^{-3}, since the total volume of the flasks was 1000 cm^{-3}. z_{L} is calculated dividing V_{s} by the circular upper surface of the soil sample. For example in the case of eolian sand and $\rho_{\mathrm{B}} = 1.40$ g cm^{-3} V_{s} is 71.4 cm^3, the soil surface π 4.59^2 cm^2, and z_{L} 1.08 cm.

Equation (15) was solved for $k_{\mathrm{s}}{\cdot}\Theta_{\mathrm{a}}$ by starting the right hand side with an initial ζ_0 based on an $(k_{\mathrm{s}}{\cdot}\Theta_{\mathrm{a}})_0 = k_{\mathrm{H}}\, V_{\mathrm{H}}/V_{\mathrm{s}}$, that is, obtained by equating the right- and left-hand side of inequality (6). Six iterations suffice to reduce the incremental change well below 1% for all Θ_{w}. The dependence on soil moisture content of the resulting $k_{\mathrm{s}}{\cdot}\Theta_{\mathrm{a}}$ is shown in Fig. 2 along with that for the original estimate $(k_{\mathrm{s}}{\cdot}\Theta_{\mathrm{a}})_0$. For the later comparison with the data from Smith-Downey et al. (2006) the soil moisture is given as water saturation $S = \Theta_{\mathrm{w}}/\Theta_{\mathrm{p}}$ rather than Θ_{w}.

The major result of our recalculation of $k_{\mathrm{s}}{\cdot}\Theta_{\mathrm{a}}$ is that the correction introduced by $\overline{M_{\mathrm{S}}}/M_{\mathrm{H}}$ is small. That is—for the measurements presented—$\overline{M_{\mathrm{S}}}/M_{\mathrm{H}}$ does not deviate too much from unity for most $\Theta_{\mathrm{w}}/\Theta_{\mathrm{p}}$. The reason is, of course, that for the given choice of soil parameters ζ is large, larger than z_{L} for most cases (see Fig. 3 which gives examples for $\overline{M_{\mathrm{S}}}/M_{\mathrm{H}}$ and ζ as a function of $\Theta_{\mathrm{w}}/\Theta_{\mathrm{p}}$). Exceptions occur in the curves for $k_{\mathrm{s}}(\Theta_{\mathrm{w}}/\Theta_{\mathrm{p}}){\cdot}\Theta_{\mathrm{a}}$ for the upper limits of the respective ρ_{B} and here only for the data points of highest soil moisture (Fig. 2, panels a and b). These values for ρ_{B} generate Θ_{p} which are probably unrealistically low and cause distortions for high $\Theta_{\mathrm{w}}/\Theta_{\mathrm{p}}$.

The smallness of the corrections means that the original shape of the soil moisture dependence of k_{H} from Fig. 1 (panels c and d) remains preserved in $k_{\mathrm{s}}{\cdot}\Theta_{\mathrm{a}}$ if the latter were plotted against the soil moisture content in units of % w/w. It is the switch to $\Theta_{\mathrm{w}}/\Theta_{\mathrm{p}}$ for soil moisture that introduces changes in the form of $k_{\mathrm{s}}(\Theta_{\mathrm{w}}/\Theta_{\mathrm{p}}){\cdot}\Theta_{\mathrm{a}}$, namely a compression or dilation of $k_{\mathrm{s}}(\Theta_{\mathrm{w}}/\Theta_{\mathrm{p}}){\cdot}\Theta_{\mathrm{a}}$ along the abszissa depending on the assumed Θ_{p}. The choice of ρ_{B} also impacts the amplitude of $k_{\mathrm{s}}(\Theta_{\mathrm{w}}/\Theta_{\mathrm{p}}){\cdot}\Theta_{\mathrm{a}}$ since it influences V_{s}. Fig. 2 serves to demonstrate the range of possible choices for $k_{\mathrm{s}}(\Theta_{\mathrm{w}}/\Theta_{\mathrm{p}}){\cdot}\Theta_{\mathrm{a}}$. It is altogether moderate.

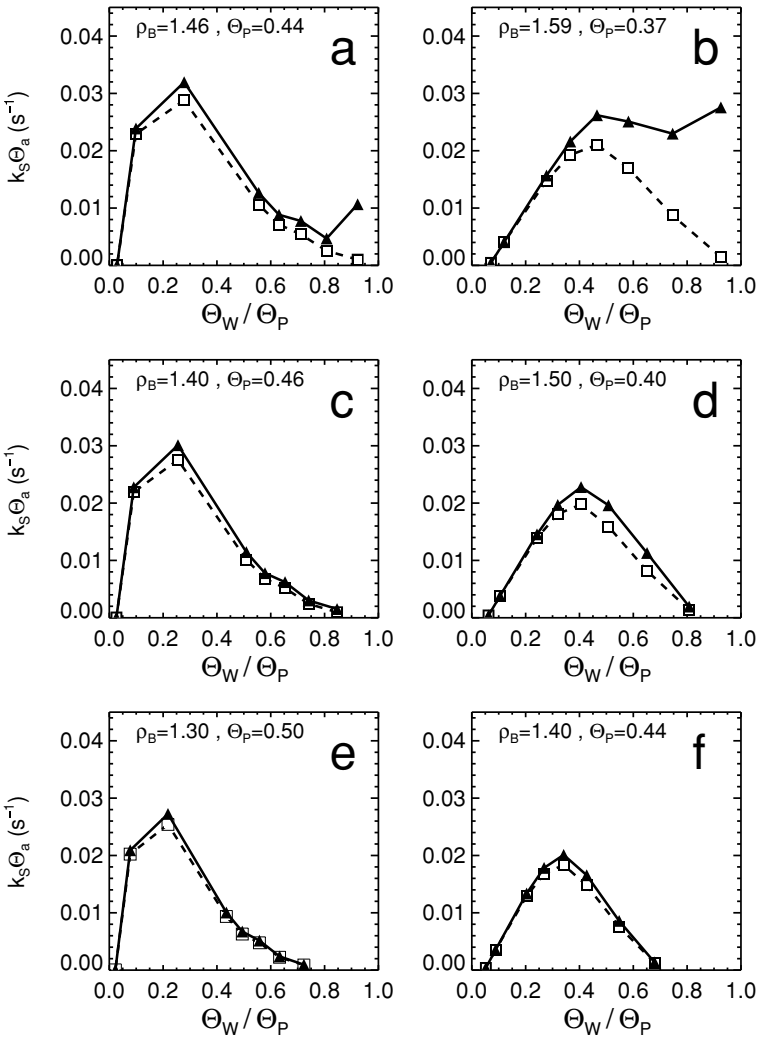

Fig. 2. H_2 uptake rate constants in soil, $k_s \cdot \Theta_a$, as a function of soil moisture for eolian sand (panels a, c, e) and loess loam (panels b, d, f). $k_s \cdot \Theta_a$ is derived from the data in Fig. 1 (panel c, no treatment, for eolian sand; panel d for loess loam) for various choices of bulk density, ρ_B, and total pore volume, Θ_P. Open squares represent the uncorrected $(k_s \cdot \Theta_a)_0 = k_H \cdot V_H / V_s$. The full triangles represent $k_s \cdot \Theta_a$ corrected for the decrease in the mixing ratio of H_2 in soil. See text for details.

In particular, the respective forms of $k_s(\Theta_w/\Theta_p)\cdot\Theta_a$ for eolian sand and loess loam remain preserved for the different parameter choices but quite distinct from each other. In the following, we will assume that panels (c) and (d) represent the most plausible choices for $k_s(\Theta_w/\Theta_p)\cdot\Theta_a$ for eolian sand and loess loam. Padé functions were used for a numerical fit to the recalculated data points in panel (c) and (d). This choice has no physical background except that these functions a priori well approximate the observed form of the moisture dependence. For the fit a Levenberg-Marquardt least-squares fitting procedure was used. The results are

$$f_{es}\left(\frac{\Theta_W}{\Theta_P}\right) = 0.00936 \cdot \frac{\left(\frac{\Theta_W}{\Theta_P} - 0.02640\right)\cdot\left(1 - \frac{\Theta_W}{\Theta_P}\right)}{\left(\frac{\Theta_W}{\Theta_P}\right)^2 - 0.1715\cdot\left(\frac{\Theta_W}{\Theta_P}\right) + 0.03144} \quad (20)$$

for eolian sand, and

$$f_{ll}\left(\frac{\Theta_W}{\Theta_P}\right) = 0.01997 \cdot \frac{\left(\frac{\Theta_W}{\Theta_P} - 0.05369\right)\cdot\left(0.8508 - \frac{\Theta_W}{\Theta_P}\right)}{\left(\frac{\Theta_W}{\Theta_P}\right)^2 - 0.7541\cdot\left(\frac{\Theta_W}{\Theta_P}\right) + 0.2806} \quad (21)$$

for loess loam. The lower roots in the numerators of eqs. (20) and (21), 0.026 and 0.054, respectively, define the cut-off of the H_2 uptake at low moistures. The upper roots are 1 and 0.85, respectively. Outside the intervals defined by the upper and lower roots the f_i and thus $k_s(\Theta_w/\Theta_p)\cdot\Theta_a$ are zero. Figure 4 compares $f_{es}(\Theta_w/\Theta_p)$ and $f_{ll}(\Theta_w/\Theta_p)$ to the data points.

The smallness of the correction also justifies the employed correction procedure. Equation (15) assumed a cylindrically shaped soil volume, whereas the actual soil volume in the experiments was a sphere segment with a maximum depth of about 2 cm (e.g. 2.03 cm for eolian sand and $r_B = 1.40$ g cm^{-3}). The modification introduced by this simplification must be much

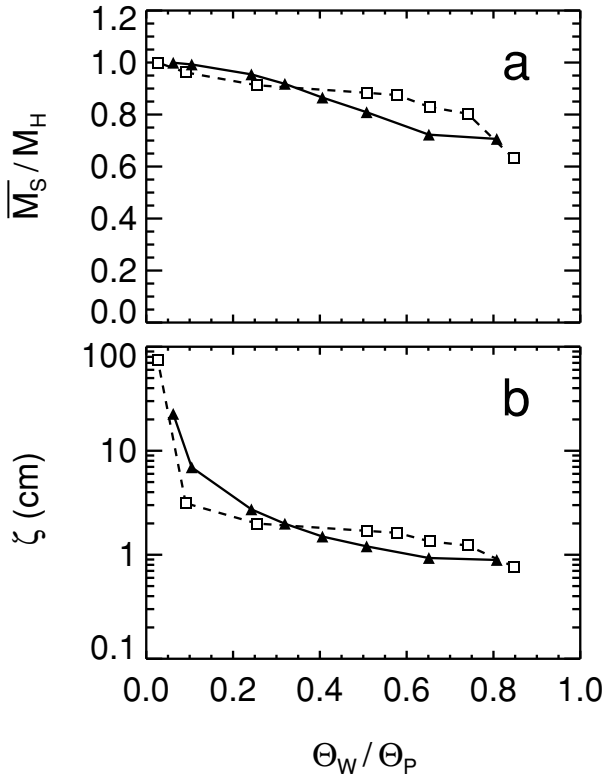

Fig. 3. Ratio of the average H_2 mixing ratio in the soil to that in the headspace, $\overline{M_S}/M_H$, as a function of soil moisture (panel a). Scale length of the H_2 decrease with soil depth, ζ, as a function of soil moisture (panel b). Open squares represent eolian sand, full triangles loess loam for the favoured pairs of ρ_B and Θ_P.

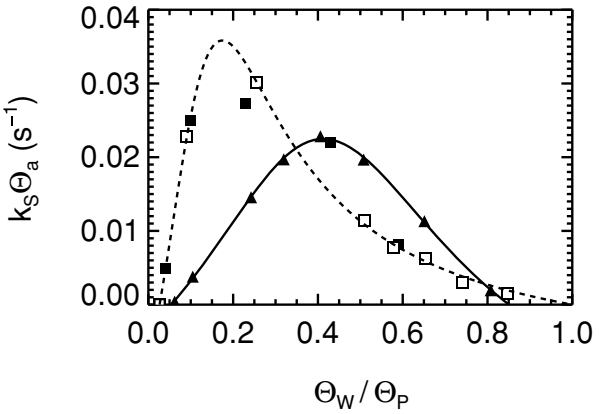

Fig. 4. Comparison of the favoured empirical $k_s \cdot \Theta_a$ from Fig. 2 for eolian sand (open squares) and loess loam (full triangles). The thin lines represent the fit functions, eqs (20) and (21). Also shown are the corrected $k_s \cdot \Theta_a$ values for boreal forest (full squares).

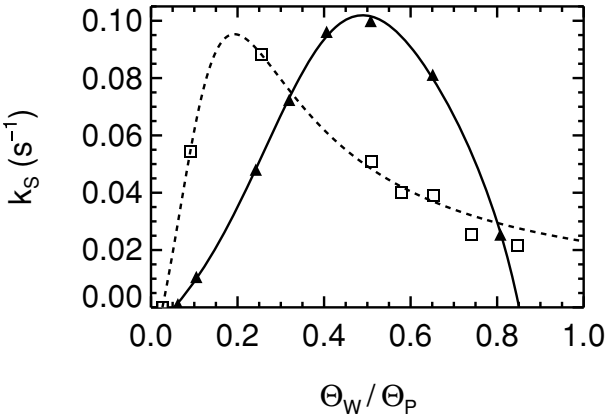

Fig. 5. H_2 removal rate constant from soil air, k_s, as function of soil moisture derived from $k_s \cdot \Theta_a$ in Fig. 4. Open squares: eolian sand; full triangles: loess loam.

smaller than the calculated corrections $\overline{M_S}/M_H$ and will be considered negligible. The small size of the correction is also consistent with the observation by Conrad and Seiler (1981), that the measured k_H scaled linearly with the amount of soil used in the experiment over a range of 20–120 g.

Since Θ_a is known, we can also derive $k_s(\Theta_w/\Theta_p)$ from the $k_s(\Theta_w/\Theta_p)\cdot\Theta_a$ in Fig. 2. It is shown in Fig. 5 for the selected cases. The systematic difference between eolian sand and loess loam seen in $k_s(\Theta_w/\Theta_p)\cdot\Theta_a$ is equally evident for $k_s(\Theta_w/\Theta_p)$. In the case of eolian sand the decay of k_s towards high Θ_w/Θ_p flattens out and ends in a finite value of k_s virtually up to $\Theta_w/\Theta_p = 1$ when all pores are filled with water. This indicates that in this case high soil moistures do not completely block the access of H_2 to the active removal sites. In contrast, for loess loam that decay remains steep and k_s appears to reach zero at Θ_w/Θ_p below 0.9.

The two curves for $k_s(\Theta_w/\Theta_p)$ also differ at low Θ_w/Θ_p. For eolian sand the increase towards the maximum starts earlier and is steeper than that for loess loam. As a consequence $k_s(\Theta_w/\Theta_p)$ for loess loam reaches the maximum at higher Θ_w/Θ_p. These differences indicate that not only the total porosity, Θ_p, but also the size distribution of the pores must play a role in determining $k_s(\Theta_w/\Theta_p)$. This subject will be taken up in the discussion, Section 4. Here, we only note that the mean lifetime of H_2 in soil which is given by

$$\tau = k_s^{-1} \tag{22}$$

is at least 10 s in both soils. This indicates that the removal reaction of an H_2 molecule on the internal soil surface must be a rare event. Assuming a typical diameter of 30 μm for a pore, which seems appropriate for eolian sand, less than 1 collision in 10^8 of an H_2 molecule with the surrounding pore surface will lead to its subsequent uptake.

2.2. *Reanalysis of the flow experiments*

The flow experiments too determine the entity, $k_s \cdot \Theta_a$, rather than k_s directly. With the assumption of a uniform removal rate

constant the H_2 mixing ratio in the flow decreases exponentially as the air moves through the soil plug. The characteristic time constant is

$$k_S \cdot \Theta_a = -\ln\left(\frac{M_{out}}{M_{in}}\right) \cdot \frac{f}{V_S}, \tag{23}$$

where f is the volume flow rate of air and V_s the volume of the soil plug. The numerical values of these and M_{in}, the H_2 mixing ratio of the incoming air were given in Section 2. The outgoing mixing ratio, M_{out}, was calculated from the H_2 uptake rate, U_{H2}, given by Smith-Downey et al. (2006) (see also Fig. 1) and eq. (1). The resulting $k_s(\Theta_w/\Theta_p)\cdot\Theta_a$ for boreal forest soil (and $T = 23^\circ$C) is also shown in Fig. 4. Obviously, its pattern remains quite close to that of the original data on U_{H2} (Fig. 1, panel f), and falls between those for the data for eolian sand and loess loam.

3. Dependence on soil temperature

Unlike soil moisture, which strongly acts also on soil properties, such as diffusivity, P, or the air volume fraction, Θ_a, the soil temperature, T, essentially acts only on the enzyme activity itself with a small correction owing to the T dependence of molecular diffusivity. Thus the removal rate constant of H_2 in soil, k_s, differs only by a virtually constant, temperature independent, factor from the measured variable, whether removal rate constant in the head space, k_H, deposition velocity, v_d, or a properly defined removal rate, U_{H2}. As a consequence, there is no need for a reanalysis of the published data to establish the temperature dependence of k_s, $k_s(T)$. In addition more of the original data remain usable.

The available data on $k_s(T)$ are summarized in Fig. 6. Since the original data are given in different units and since we are only interested in the functional form of this dependence, the data were normalized by assigning the value 1 to the maximum removal rate in each data set. The scaling factors and the original units are given in the figure caption along with the origin or type of soil. For the flow experiment data from Smith-Downey et al. (2006), the reanalyzed values were used. Despite a considerable scatter all the data follow the same general pattern: zero removal at temperatures below -20°C and above 80°C, and a broad maximum peaking around 30°C. Much of the data below 30°C and virtually all below 0°C are from Smith-Downey et al. (2006). These data clearly demonstrate that k_s remains finite well below 0°C, the freezing point of water, and approaches zero only at about -20°C. A systematic difference between the various soils cannot be discerned. The decrease in $k_s(T)$ at low temperatures is well approximated by a Fermi distribution (Smith-Downey et al. 2006). A corresponding fit to the present data for $T \leq 40^\circ$C yields

$$g_1(T) = \frac{1}{1 + \exp[-(T - 3.8)/6.7]}. \tag{24}$$

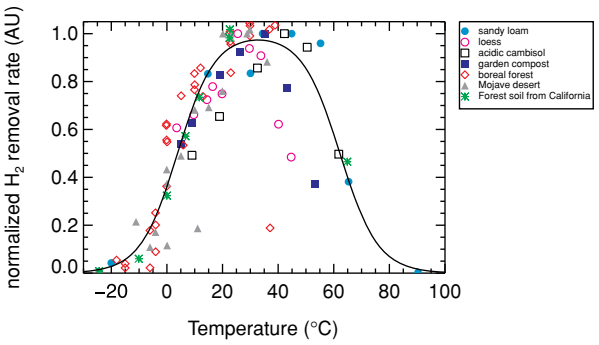

Fig. 6. Removal rate constant of H_2 in soil as a function of the temperature. The data are from various authors. Full circles: sandy loam from Aikin County, SC, USA; original units: min^{-1} (removal rate constant); scaling factor: 0.2395 (Fallon, 1982). Open circles: loess from the vicinity of Mainz, Germany; original units: 10^{-2} cm/s (nominal deposition velocity); scaling factor: 0.1453 (Liebl and Seiler, 1976). Full squares: garden compost soil, greenhouse, University of Konstanz, Germany; original units: nl H_2 min^{-1} g^{-1} (removal rate per g soil); scaling factor: 1.194 (Schuler and Conrad, 1991). Open squares: acidic cambisol from Mainau Forest near Konstanz, Germany; original units: nl H_2 min^{-1} g^{-1} (removal rate per g soil); scaling factor: 0.2200 (Schuler and Conrad, 1991). Asteriks: Forest soil from California, USA; instead of the original units: pmol cm^{-3} s^{-1} (removal rate per cm^3 soil) we used the reanalyzed $k_s\cdot\Theta_a$ for all of the following data from Smith-Downey et al. (2006). Open diamonds: boreal forest soil near Delta Junction, Alaska, USA for soil moistures of 4, 10, 23, 43 and 59% saturation; scaling factor: 1.00 Full triangles: Mojave desert soil for soil moistures of 11, 19, 32 and 46% saturation; scaling factor: 1.00. The heavy line represents the fit by $g(T)$, cf. eqs (24) and (25).

The fit parameter, $T_{1/2} = 3.8^\circ$C, underlines that just above 0°C still $\frac{1}{2}$ of the maximum hydrogenase activity is retained. The other parameter, $T_d = 6.7^\circ$C, characterizes the slope of the distribution. Just below 0°C k_s decreases by about a factor of 2 for a temperature decrease of 5°C. The present values for $T_{1/2}$ and T_d agree reasonably well with those obtained by Smith-Downey et al. (2006).

The fact that the hydrogenase in the soil remains active below 0°C raises an interesting point. Basically, one expects an enzyme to require a liquid environment to function; transition of the surrounding water to ice should stop the hydrogenase activity. This suggests that soil hydrogenase has its own microenvironment that does not freeze at 0°C—for example the interior of a cell which contains organic molecules which suppress freezing—which may be taken as a point in favour for the uptake by living bacteria.

Due to the sparser and more scattered data the decrease in $k_s(T)$ at higher temperatures is less well defined. It also appears that the upper flank of the temperature dependence varies systematically with the type or regional origin of the soil. In fact, Fallon (1982) had already suggested that the T optimum of the hydrogenase activity might adapt to the local climate, that is, occur at a higher temperature when the climate is warmer.

Nevertheless this flank ($T \geq 40^{\circ}$C) can also be approximated by a Fermi distribution:

$$g_2(T) = \frac{1}{1 + \exp[+(T - 62.2)/7.1]}. \quad (25)$$

Besides the large scatter there is another problem with the data at higher temperatures. It is not clear from the experiments included in Fig. 1, whether the temperature dependence is free of hysteresis, in particular whether the soil returns to its former removal rates at lower temperatures once a temperature threshold has been exceeded. Most papers make no statement to that effect. The exception is Liebl and Seiler (1976), who state that heating to 45°C did not change the removal rates at lower temperatures. This is in contrast to the observation by Förstel (1986), who states for his measurements of v_d in undisturbed soil using tritiated hydrogen, HT, that above about 40°C the HT uptake is lowered irreversibly. This latter observation is confirmed by a recent paper by Chowdhury and Conrad (2010), who investigated various soils and found that at least part of the soil hydrogenases is deactivated irreversibly at relatively low temperatures (>30°C) and short exposure times.

Clearly the T dependence of k_s at above 40°C is not as well defined as one might wish and could well deviate from that suggested by eq. (25). To provide a complete fit to the present data on $k_s(T)$ we use the function

$$g(T) = g_1(T) + g_2(T) - 1, \quad (26)$$

where $g_1(T)$ represents the low temperature flank of the T dependence of k_S and $g_2(T)$ the high temperature flank. $g(T)$ is shown in Fig. 6 and should approximate $k_s(T)$ reasonably well for temperatures <40°C. When applied to temperatures >40°C the caveats above should be borne in mind.

4. Discussion

In the diffusion eq. (7) the removal rate constant for H_2 in soil air, k_s, is associated with Θ_a, the air filled pore volume fraction. Consequently, in any solution of eq. (7) k_s and Θ_a will always appear as the product $k_s \cdot \Theta_a$. Thus our primary goal is the term $k_s \cdot \Theta_a$ and its dependence on soil moisture and temperature, although much of the following discussion will centre on k_s.

Since the dependences of $k_s \cdot \Theta_a$ on soil moisture and temperature are separable (Smith-Downey et al., 2006) the combined dependence is given by

$$k_S(\Theta_W/\Theta_P, T) \cdot \Theta_a = A \cdot f_i(\Theta_W/\Theta_P) \cdot g(T), \quad (27)$$

where f_i is defined by eq. (20) or eq. (21) and $g(T)$ by eq. (26). A is a fitting parameter to account for different amounts of hydrogenase in the soil under investigation. The terms in eq. (27) have limited applicability ranges. As far as the temperature dependence is concerned only the low temperature branch $g_1(T)$, eq. (24), can claim with some reason to be applicable for all soils. The high temperature branch, $g_2(T)$, depends on the type of soil; the average given by eq. (25) is only a rough overall approximation. Fortunately, this is less of a handicap for the calculation of the soil uptake rate as it may seem. In nature soil temperatures above 40°C will in many cases be associated with very dry soils. In these cases the uptake will be limited anyway by a very low $k_s(\Theta_w/\Theta_p)\cdot\Theta_a$ (Fig. 4) and the temperature influence is of little consequence.

As Fig. 4 demonstrates the moisture dependence, $k_s(\Theta_w/\Theta_p)\cdot\Theta_a$, varies also with the type of soil. We will argue below that this variation is mainly caused by the size distribution of the soil pores, which in turn is caused by the size distribution of the soil particles. If this is correct the form of $k_s(\Theta_w/\Theta_p)\cdot\Theta_a$ should vary within a rather moderate range only. The eolian sand studied by Conrad and Seiler (1981) had a median grain diameter, ϕ, of about 200 μm and a narrow size distribution, in contrast their loess loam sample had a median ϕ of about 20 μm and a much wider size distribution (cf. Seiler et al., 1977). Most soils responsible for H_2 uptake should fall between these two extremes. Thus for most soils, the curves for $k_s(\Theta_w/\Theta_p)\cdot\Theta_a$ should fall between the two examples shown in Fig. 4.

It is instructive to analyse the shape of $k_s(\Theta_w/\Theta_p)\cdot\Theta_a$ a little more closely—beyond the general observations made in Section 2. The contribution from the factor Θ_a is straightforward. It superimposes a linear decrease on k_s with $\Theta_a = \Theta_P$ for $\Theta_w/\Theta_P = 0$ and $\Theta_a = 0$ for $\Theta_w/\Theta_P = 1$. Hence it ensures that $k_s \cdot \Theta_a = 0$ for $\Theta_w/\Theta_P = 1$. The pattern of k_s is more complex (Fig. 5). It rests on three factors: The number of reactive sites present in the soil, their state of activation and their accessibility to soil air. The number of reactive sites (number of microorganisms or amount of hydrogenase) is fixed in a given soil sample. But the other two factors depend on soil moisture, and that in a counteracting way. On the one side water is needed to activate the hydrogenase, on the other water blocks the access to it. The activation appears to have a threshold, below which uptake vanishes, here: $\Theta_w/\Theta_P \sim 0.03$ for eolian sand and ~0.05 for loess loam. However, as the gradual increase of k_s in Fig. 5 indicates, above that threshold activation is a gradual process—not an abrupt transition. This behaviour indicates that the degree of hydrogenase activation depends on the activity of water in the soil which in turn is controlled by Θ_w/Θ_P and the size distribution of the soil pores. The capillary forces of the finer pores hold the water tightly and so lower the vapour pressure and thus water activity everywhere in the soil sample. As they are being gradually filled the resulting increase in water activity permits increased activation of the hydrogenase. Eventually, all hydrogenase in the soil is fully activated. Obviously a larger fraction of small pores means a more gradual increase in hydrogenase activation and thus in k_s as is indeed observed (see Fig. 5).

We also note that the threshold values appear to lie well below the permanent wilting points of the respective soils. These have not been measured for the present soils. The literature gives $\Theta_w/\Theta_P = 0.06$ and 0.18 for the wilting points of sand and clay loam (Scheffer and Schachtschabel, 2010). As Fig. 5

indicates, at these moistures the respective k_s have reached about 1/3 of their maximum values. Thus, when other information is lacking, a measurement of the permanent wilting point could serve as a clue for estimating the form of the rising part of k_s.

As the soil moisture increases, more and more of the reactive sites become separated from soil air by increasing layers of water molecules. Since the diffusion coefficient in water is about 4 orders of magnitude smaller than that in air, the accessibility of the reactive sites begins to diminish even as the degree of activation is still on the increase. The curve for k_s begins to turn around and eventually to decrease. That decrease is also influenced by the size distribution of pores. This is most readily visualized by realizing that the removal rate constant for an individual pore, $k_{s,i}$, must be inversely proportional to the pore radius, r_i. This $k_{s,i}$ is proportional to the number of reactive wall collisions divided by the amount of H_2 in the pore. Assuming an even distribution of the reactive sites over the pore surface $k_{s,i}$ depends on the surface to volume ratio, that is, on ${r_i}^{-1}$. The k_s for the whole soil sample is the volume weighted average over the individual $k_{s,i}$. As Θ_w/Θ_P increases the narrower pores are preferentially filled with water leaving only the larger pores with lower $k_{s,i}$ active in removing H_2. As a consequence the remaining average, k_s, decreases with Θ_w/Θ_P and the exact form of that decrease will depend on the size distribution of the pores. With the assumptions made here, however, k_s should always end with a finite value for $\Theta_w/\Theta_P = 1$.

The empirical curves for k_s in Fig. 5 do not quite extend to $\Theta_w/\Theta_P = 1$ and the part between $\Theta_w/\Theta_P \sim 0.8$ and 1 must be extrapolated. In the case of eolian sand that extrapolation appears to lead to a finite value of k_s for $\Theta_w/\Theta_P = 1$, which is compatible with the explanation above. In the case of loess loam the straightforward extrapolation leads to a $k_s = 0$ for $\Theta_w/\Theta_P \sim 0.9$. This would not be compatible with the arguments above, and if eventually found correct will need additional explanation. A simple explanation would be that the surface distribution of the reactive sites is not uniform over all pore sizes but excludes the largest pores.

For the practical problem of calculating the deposition velocity, v_d, the exact form of k_s for $\Theta_w/\Theta_P > 0.9$ is of little consequence. In the present context v_d is well approximated (Yonemura et al., 2000a) by

$$v_d = \sqrt{k_s \cdot \Theta_a \cdot P}. \tag{28}$$

Since both, soil diffusivity, P, and air filled pore volume fraction, Θ_a, are very small in that soil moisture range, v_d will be extremely small in any case.

The recognition that k_s depends on the pore size distribution, however, raises another question. Namely, whether the laboratory experiments, in all of which the soils were somehow manipulated, maintained the size distribution well enough, such that their results are applicable for the respective soils in their natural setting. Of particular interest is the applicability of the functional form of the dependence of $k_s \cdot \Theta_a$ on soil moisture. (As we argued earlier the functional form of the temperature dependence should not be influenced by the soil structure.) There are three points that speak for such an applicability. (1) The difference in the form of $k_s(\Theta_w/\Theta_p)\cdot\Theta_a$ for eolian sand and loess loam, as found here, is only moderate, even though their median particle diameter and consequently their pore sizes differ by an order of magnitude. Thus we expect that the much smaller differences introduced by the manipulation of the soils has little impact on the $k_s(\Theta_w/\Theta_p)\cdot\Theta_a$ of the soil samples. (2) For eolian sand, a loose soil, manipulation should have little impact on pore size distribution anyway. Even for loess loam where it is possible that the pore size distribution was changed the change should be limited to the range of the wider pores. Since most of the soil consists of aggregated particles, the distribution of the finer pores should remain unchanged. That is, even for loess loam a possible impact on $k_s(\Theta_w/\Theta_P)$ should be limited to large Θ_w/Θ_P. (3) The headspace experiments in principle also measure v_d. The deposition velocities derived for the parameter choices given in panels c, d of Fig. 2 and for the maximum in $k_s \cdot \Theta_a$ are 0.07 cm s^{-1} for eolian sand, and 0.04 cm s^{-1} for loess loam. They closely agree with the corresponding v_d measured by earlier field experiments on the same soils in natural setting (Seiler et al., 1977). This may be taken as additional, circumstantial evidence in support of the notion that the two laboratory profiles of $k_s(\Theta_w/\Theta_P)$ recommended here (Fig. 4) are reasonably applicable to the respective soils in the field. At the same time we should remain aware of the fact that each of these profiles has its own uncertainty introduced by the uncertainties of the assumed ρ_B and Θ_p as illustrated in Fig. 2.

So far only the two soils, eolian sand and loess loam, came with enough data and auxiliary information to allow a reanalysis and to determine a well defined uptake rate constant of H_2 in soil and its dependence on moisture, $k_s(\Theta_w/\Theta_P)\cdot\Theta_a$. Although the $k_s(\Theta_w/\Theta_P)\cdot\Theta_a$ for both soils exhibit the same general pattern, the exact form appears to depend on the type of soil, in particular on the size distribution of the soil pores, respectively of the soil particles. There may be other factors at work. Soil pH has been shown to influence the H_2 uptake rate (Fallon, 1982; Guo and Conrad, 2008), but the influence of soil pH on $k_s(\Theta_w/\Theta_p)\cdot\Theta_a$ has not been investigated so far. Another factor possibly influencing $k_s(\Theta_w/\Theta_p)\cdot\Theta_a$ is the content of soil organic carbon. Again no data are available. Clearly more laboratory measurements of $k_s(\Theta_w/\Theta_P)\cdot\Theta_a$ are needed to identify such factors and to more completely cover the range of soil types primarily responsible for the global uptake of H_2.

For some soils, for example, sandy loam and loamy sand, whose $k_s(\Theta_w/\Theta_P)\cdot\Theta_a$ would tend to fall between those of eolian sand and loess loam, appropriately weighted superpositions of those two curves (Fig. 4) could serve as a good approximation even now.

The considerations above offer some guidelines on the information these experiments should provide to ensure comparability and systematic interpretation of their results. These include: specification of the type of soil along with a reasonably complete characterisation of soil properties, notably Θ_p, ρ_B, permanent wilting point, grain size distribution if feasible, and content of organic carbon. Moreover, the measurements should extend over the full range of $0 \leq \Theta_w/\Theta_P \leq 1$ and be spaced with reasonable density for a better definition of $k_s(\Theta_w/\Theta_P)\cdot\Theta_a$. The evaluation of the headspace experiments would also benefit from a simpler geometry of the soil volume, that is, a cylindrical shape. In addition, it would be useful to have flow experiments on segments of intact soil cores to directly compare the data from manipulated soils to those of soils in their original setting. Finally, it might be useful to study also individual grain size fractions to test whether the distribution of hydrogenase is uniform across all pore sizes or not, as seems indicated for loess loam.

5. Summary and conclusions

Our reanalysis showed that existing laboratory measurements, in particular the headspace experiments by Conrad and Seiler (1981), allow to quantitatively deduce the dependence of the rate constant for H_2 uptake in soil on soil moisture, $k_s(\Theta_w/\Theta_P)$. Actually it determines the product $k_s(\Theta_w/\Theta_P)\cdot\Theta_a$, where Θ_a is the air-filled pore volume fraction. For two soils, eolian sand and loess loam, the functional form of $k_s(\Theta_w/\Theta_P)\cdot\Theta_a$ could be specified. The reanalysis maintains the generally accepted qualitative form, zero uptake at very low and high moistures and a maximum in between, but modifies the details. The $k_s(\Theta_w/\Theta_P)\cdot\Theta_a$ of the two soils differ. This difference can be explained on the basis of the difference in pore size distribution.

For the temperature dependence $k_s(T)$ or $k_s(T)\cdot\Theta_a$ more laboratory data on a wider variety of soils are available, notably those by Smith-Downey et al. (2006). $k_s(T)$ shows a broad maximum around 30°C and zero uptake below −20°C and above 80°C. The decrease to lower temperatures is reasonably uniform for all soils investigated and can be approximated by a Fermi distribution (Smith-Downey et al., 2006). The upper flank can also be approximated by a Fermi distribution but is less well defined. It appears that it may vary with the type or regional origin of the soil.

As Smith-Downey et al. (2006), have already pointed out on the basis of their experiments the combined dependence $k_s(\Theta_w/\Theta_P,T)\cdot\Theta_a$ can be described by the product of the separate dependences on T and Θ_w/Θ_P.

The functional forms of $k_s(\Theta_w/\Theta_P,T)\cdot\Theta_a$ should be applicable to the respective soils in the field, but may be subject to further modifications by varying contents in organic carbon and varying soil pH. To establish the latter influence more laboratory work is required for which we suggest some auxiliary measurements to facilitate a more accurate and systematic interpretation.

References

Chowdhury, S.P. and Conrad, R. 2010. Thermal deactivation of high-affinity H_2 uptake in soils. *Soil Biol. Biochem.* **42**, 1574–1580, doi:10.1016/j.soilbio.2010.05.027.

Conrad, R. 1999. Soil microorganisms oxidizing atmospheric trace gases (CH_4, CO, H_2, NO). *Indian J. Microbiol.* **39**, 193–203.

Conrad, R. and Seiler, W. 1981. Decomposition of atmospheric hydrogen by soil-microorganisms and soil enzymes. *Soil Biol. Biochem.* **13/1**, 43–49.

Conrad, R and Seiler, W. 1985. Influence of temperature, moisture, and organic carbon on the flux of H_2 and CO between soil and atmosphere: field studies in subtropical regions. *J. Geophys. Res.* **90**, 5699–5709.

Constant, P., Chowdury, S.P., Pratscher, J., and Conrad, R. 2010. Streptomycetes contributing to atmospheric molecular hydrogen soil uptake are widespread and encode a putative high- affinity [NiFe]-hydrogenase. *Environ. Microbiol.* **12**, 821–829, doi:10.1111/j.1462-2920.2009.0230.x.

Ehhalt, D.H. and Rohrer, F. 2009. The tropospheric cycle of H_2: a critical review. *Tellus* **61B**, 500–535, doi:1111/j.1600-0889.2009.00416.x.

Fallon, R.D. 1982. Influences of pH, temperature, and moisture on gaseous tritium uptake in surface soils. *Appl. Environ. Microbiol.* **44**, 171–178.

Förstel, H. 1986. Uptake of elementary tritium by the soil. *Radiat. Prot. Dosim.* **16**, 75–81.

Guo, R. and Conrad, R. 2008. Extraction and characterization of soil hydrogenases oxidizing atmospheric hydrogen. *Soil Bio. Biochem.* **40**, 1149–1154, doi:10.1016/j.soilbio.2007.12007.

Hauglustaine D.A. and Ehhalt D.H. 2002. A three-dimensional model of molecular hydrogen in the troposphere. *J. Geophys. Res.* **107**, 4330, doi:10.1029/2001JD001156.

Liebl, K.H. and Seiler, W. 1976. CO and H_2 destruction at the soil surface. In: *Production and Utilisation of Gases* (eds H.G. Schlegel, G. Gottschalk, and N. Pfenning) E. Goltze KG Göttingen, Germany, 215–229.

Millington, R.J. and Quirk, J.M. 1961. Permeability of porous solids. *Trans. Faraday Soc.* **57**, 1200–1207.

Novelli, P. C., Lang, P.M., Masarie, K.A., Hurst, D.F., Myers, R. and Elkins, J.W. 1999. Molecular hydrogen in the troposphere: global distribution and budget. *J. Geophys. Res.* **104**: 30427–30444.

Price, H., Jaegle, L., Rice, A., Quay, P., Novelli, P.C. and Gammon, R. 2007. Global budget of molecular hydrogen and its deuterium content: constraints from ground station, cruise, and aircraft observations. *J. Geophys Res.* **112**, D22108, doi:10.1029/2006JD008152.

Rhee, T.S., Brenninkmeijer, C.A.M. and Röckmann, T. 2006. The overwhelming role of soils in the global atmospheric hydrogen cycle. *Atmos. Chem. Phys.* **6**, 1611–1625.

Sanderson, M.G., Collins, W.J., Derwent, R.G. and Johnson, C.E. 2003. Simulation of global hydrogen levels using a Lagrangian three-dimensional model. *J. Atmos. Chem.* **46**(1), 15–28.

Scheffer, F. and Schachtschabel, P. 2010. *Lehrbuch der Bodenkunde*, 16. Auflage, Spektrum, Akademischer Verlag, Heidelberg.

Schmitt, S., Hanselmann, A., Wollschläger, U., Hammer, S. and Levin, I. 2009. Investigation of parameters controlling the soil sink of atmospheric molecular hydrogen. *Tellus* **61B**, 416–423, doi:10.1111/j.1600-0889.2008.00402.x.

Schuler, S. and Conrad, R. 1990. Soils contain two different activities for oxidation of hydrogen. *FEMS Microbiol. Ecol.* **73**, 77–84.

Schuler, S. and Conrad, R. 1991. Hydrogen oxidation activities in soil as influenced by pH, temperature, moisture, and season. *Biol. Fertility Soils* **12**, 127–130.

Schultz, M.G., Diehl, T., Brasseur, G.P. and Zittel, W. 2003. Air pollution and climate-forcing impacts of a global hydrogen economy. *Science* **302**, 624–627.

Seiler, W., Liebl, K.H., Stöhr, W.Th. and Zakosek, H. 1977. CO- and H_2-Abbau in Böden. *Z. für Pflanzenernährung und Bodenkunde* **140**, 257–272.

Smith-Downey, N.V., Randerson, J.T. and Eiler, J.M. 2006. Temperature and moisture dependence of soil H_2 uptake measured in the laboratory. *Geophys. Res. Lett.* **33**, L14813, doi:10.1029/2006GL026749.

Tromp, T.K., Shia, R.-L., Allen, M., Eiler, J.M. and Yung, Y.L. 2003. Potential environmental impact of a hydrogen economy on the stratosphere. *Science* **300**, 1740–1742.

Warwick, N.J., Bekki, S., Nisbet, E.G. and Pyle, J.A. 2004. Impact of a hydrogen economy on the stratosphere and troposphere studied in a 2-D model. *Geophys. Res. Lett.* **31**, L05107, doi:10.1029/2003GL019224.

Yonemura, S., Kawashima, S. and Tsuruta, H. 1999. Continuous measurements of CO and H_2 deposition velocities onto an andisol: uptake control by soil moisture *Tellus* **51B**, 688–700.

Yonemura, S., Kawashima, S. and Tsuruta, H. 2000b. Carbon monoxide, hydrogen, and methane uptake by soils in a temperate arable field and a forest. *J. Geophys. Res.* **105**, 14347–14362.

Yonemura, S., Yokozawa, M., Kawashima, S. and Tsuruta, H. 2000a. Model analysis of the influence of gas diffusivity in soil on CO and H_2 uptake, *Tellus* **52B**, 919–933.